

Techniques for Minimizing Error Propagation in Decision Feedback Detectors for Recording Channels

Fang Zhao, George Mathew, and B. Farhang-Boroujeny

Abstract—Decision feedback equalization (DFE) is a low-cost approach for signal detection in magnetic recording channels. However, it suffers from the phenomenon of error propagation (EP). In this paper, two approaches are proposed for minimizing EP in DFE. The first approach imposes appropriate constraints on the feedback equalizer. The second approach uses simple threshold techniques to detect the presence of decision errors and to either correct these errors or minimize the possibility of further errors. Computer simulations show that the proposed techniques reduce EP very significantly. Theoretical analyses of the threshold techniques are presented to quantify the associated false and correct detection probabilities. By combining the analysis with an existing EP simulation method, a fast simulation procedure is derived for estimating EP and bit error rate (BER).

Index Terms—Decision feedback equalization, DFE, error propagation, magnetic recording.

I. INTRODUCTION

PERFORMANCE and complexity are two important figures of merit that are used for assessing a detector. Decision feedback equalization (DFE) detectors are known for their simple structure and, hence, cost effectiveness while offering satisfactory performance. As a result, recent years have witnessed a renewed interest in DFE-type detectors for magnetic recording applications and several novel modifications have been proposed to improve performance, e.g., fixed-delay tree search with decision feedback (FDTS/DF) [1], dual DFE [2], and multilevel DFE (MDFE)[3]. A concern that is common to all decision feedback-based approaches is the phenomenon of error propagation (EP). To understand this, refer to Fig. 1, which shows the schematic of the conventional DFE detector. The forward equalizer suppresses the precursor intersymbol interference (ISI), i.e., from bits that are not yet detected, and channel noise while the feedback equalizer suppresses the postcursor ISI, i.e., from bits that are already detected, using past decisions. Hence, erroneous past decisions will result in residual postcursor ISI at the slicer input that can possibly cause further decision errors, thus resulting in EP. In this paper, we study the phenomenon of EP in conventional DFE in magnetic recording applications and propose techniques for minimizing it. The principles behind these techniques are also applicable to data communication channels.

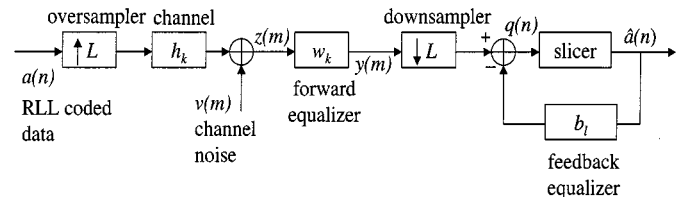


Fig. 1. Discrete-time model of the magnetic recording channel with decision feedback detection scheme (L is the oversampling factor).

EP can be characterized using burst-length distribution (BLD), i.e., cumulative-probability distribution of error bursts as a function of burst length. The faster this distribution decays, the lesser is the extent of EP and vice versa. Hence, aim of any EP reduction technique should be to reduce the probability of long error bursts so that the requirement on error-control coding (ECC) can be relaxed. Two approaches may be adopted to develop such techniques. One approach is to appropriately modify the design of equalizer, detector, and/or the run-length-limited (RLL) coding scheme so that the probability of long bursts is reduced. Another approach is to develop special strategies to detect the presence of decision errors and take measures to prevent further errors. In this paper, we adopt a combination of both these approaches.

In recent years, several researchers proposed techniques for minimizing EP in DFE-type detectors. Russul and Bergmans [4] proposed a technique by combining DFE with partial response precoding and detection for reducing EP in an M -ary system. Use of erasures (i.e., samples that lie near to the decision thresholds) in reducing EP was reported by Chiani [5]. Replacing an unreliable decision by a temporary decision and correcting the latter based on the decision at the next instant was proposed by Fertner [6] for reducing EP in DFE. Techniques for minimizing EP in MDFE were proposed by Mathew *et al.* [7], Ueno *et al.* [8], [9], and Likhanov *et al.* [10]. Mathew *et al.* [7] developed threshold techniques for detecting the presence of erroneous decisions and changed the slicer threshold appropriately to prevent further decision errors. Ueno *et al.* [8], [9] proposed to change the slicer threshold appropriately whenever the detected bit stream violates the code constraints or when the accumulated gain-error signal or dc-error signal exceeds some threshold. Likhanov *et al.* [10] proposed a three-step approach. First, detection of error bursts is done using four simple threshold tests at the slicer input. Second, upon detection of a burst, a time-varying offset is added to the slicer input to prevent further decision errors. Third, reliability of the resulting

Manuscript received February 4, 2000; revised May 31, 2000.

F. Zhao and B. Farhang-Boroujeny are with the Department of Electrical Engineering, National University of Singapore, Singapore 117596.

G. Mathew is with the Coding and Signal Processing Department, Data Storage Institute, Singapore 117608.

Publisher Item Identifier S 0018-9464(01)00617-3.

decisions is assessed by evaluating an appropriate energy function. Very recently, Lin *et al.* [11] reported a threshold-based method for minimizing EP in M3DFE, an advanced version of MDFE.

In this paper, we propose two approaches for minimizing EP in DFE: 1) equalizer design with appropriate constraints on feedback equalizer taps and 2) simple threshold techniques to detect the presence of decision errors and to prevent further errors. Compared to the energy-constrained approach proposed in [12], the magnitude-constrained design proposed in this paper can more effectively suppress longer error events. Theoretical analysis has been carried out to quantify the false and correct detection probabilities associated with the threshold techniques. By combining the results of this analysis with an existing fast prediction algorithm [14], a fast approach is developed for estimating the overall BLD and/or bit error rate (BER) of the detector when the threshold techniques are applied. This paper is organized as follows. The constrained equalizer design procedure is presented in Section II. The threshold methods are presented in Section III. Theoretical analysis of the threshold methods are presented in Section IV. Simulation results are presented in Section V and the paper concludes in Section VI.

II. CONSTRAINED EQUALIZER DESIGN FOR DFE

In this section, we describe the equalizer design for DFE with some special constraints on the feedback equalizer taps for controlling EP.

Consider the block schematic shown in Fig. 1. Here, $a(n)$ is the RLL rate 16/17 (0,6/6) coded data in ± 1 format (i.e., write-current polarity) and h_k is the sampled bit response of the recording channel. The forward equalizer w_k , $k = 0, 1, \dots, N_f - 1$, is a fractionally spaced finite-impulse response (FIR) filter with tap spacing T/L , where T and L are the channel bit duration and oversampling factor, respectively, and $b_l, l = 1, 2, \dots, N_b$, are the T -spaced feedback equalizer taps. The channel bit response is given by $h_k = \tilde{h}_k - \tilde{h}_{k-L}$, where \tilde{h}_k is the step response of the channel and is modeled using the Lorentzian pulse with taps spaced at T/L given by

$$\tilde{h}_k = \frac{1}{1 + \left(\frac{2Rk}{LD_u}\right)^2}$$

where R is the code rate and D_u is the user density.¹ The channel noise $v(m)$ is assumed to be white Gaussian and its variance σ^2 is determined using the channel signal-to-noise ratio (SNR) that is defined as

$$\text{channel SNR(dB)} = 10 \log_{10} \frac{V_{op}^2}{\sigma_u^2}, \quad \sigma^2 = L\sigma_u^2/R$$

where V_{op} is the base to peak value of isolated transition response of the channel and σ_u^2 is the variance of noise in the user bandwidth.

¹User density D_u is defined as $PW50/T_u$, where $PW50$ is the pulse width of the channel step response at 50% of its peak amplitude and T_u is the duration of one user bit.

Assuming correct past decisions, the slicer input is given by

$$q(n) = \mathbf{w}^T \mathbf{z}(nL + k_0) - \mathbf{b}^T \mathbf{a}(n)$$

where $\mathbf{z}(m) = [z(m), z(m-1), \dots, z(m-N_f+1)]^T$ and $\mathbf{a}(n) = [a(n-1), a(n-2), \dots, a(n-N_b)]^T$. Here, the superscript “ T ” denotes matrix transpose, $z(m)$ is the signal at the forward equalizer input, and k_0 accounts for the delay from channel input to forward equalizer output. The forward and feedback equalizers are designed by minimizing the sum of variances of channel noise and residual ISI at the slicer input, given by

$$\begin{aligned} P_n(\mathbf{w}, \mathbf{b}) &= E[(a(n) - q(n))^2] \\ &= \mathbf{w}^T \mathbf{R}_z \mathbf{w} + \mathbf{b}^T \mathbf{R}_a \mathbf{b} + 1 - 2\mathbf{w}^T \mathbf{R}_{za} \mathbf{b} \\ &\quad - 2\mathbf{w}^T \mathbf{r}_{za} + 2\mathbf{b}^T \mathbf{r}_{aa} \end{aligned} \quad (1)$$

where $\mathbf{R}_z = E[\mathbf{z}(nL+k_0)\mathbf{z}^T(nL+k_0)]$, $\mathbf{R}_a = E[\mathbf{a}(n)\mathbf{a}^T(n)]$, $\mathbf{R}_{za} = E[\mathbf{z}(nL+k_0)\mathbf{a}^T(n)]$, $\mathbf{r}_{za} = E[\mathbf{z}(nL+k_0)a(n)]$, and $\mathbf{r}_{aa} = E[\mathbf{a}(n)a(n)]$, with $E[\cdot]$ denoting the expectation operator. All these quantities can be computed from the knowledge of the channel h_k and autocorrelations of the data $a(n)$ and the channel noise $v(m)$. Since $P_n(\mathbf{w}, \mathbf{b})$ is quadratic in \mathbf{w} and \mathbf{b} , it is straightforward to obtain the optimum values of \mathbf{w} and \mathbf{b} .

To motivate the development of constrained equalizer design for controlling EP, we proceed as follows. Let f_k denote the T -spaced equalized channel at the output of forward equalizer with the main cursor being f_0 . The slicer input can then be written as

$$q(n) = f_0 a(n) + 2 \sum_{i=1}^{N_b} b_i \epsilon(n-i) + \eta(n) \quad (2)$$

where $\epsilon(n-i) = (a(n-i) - \hat{a}(n-i))/2$ denotes the decision errors and $\eta(n)$ is the sum of channel noise and residual ISI. The residual ISI consists of precursor ISI f_k for $k < 0$, uncompensated post-cursor ISI f_k for $k > N_b$, and the mismatch between f_i and b_i for $i = 1, 2, \dots, N_b$. The term $2 \sum_{i=1}^{N_b} b_i \epsilon(n-i)$ corresponds to an undesirable offset at the slicer input due to past decision errors. Since this offset is proportional to the magnitude of feedback taps, it will be serious if the magnitude and/or the number of feedback taps are large. An immediate solution to minimize this would be to reduce the number as well as the magnitude of feedback taps. This may be accomplished in two ways, as explained below.

The tap magnitudes can be limited by imposing a constraint on the energy of the taps. That is, design the equalizers by solving the following constrained optimization problem:

$$\min_{\mathbf{w}, \mathbf{b}} P_n(\mathbf{w}, \mathbf{b}) \text{ subject to } \sum_{i=m_1}^{m_2} b_i^2 = \alpha_e \quad (3)$$

where $1 \leq m_1 \leq m_2 \leq N_b$ and α_e is a positive real number specifying the required energy. This idea of using energy constraint for minimizing EP was first proposed by Mathew *et al.* [12]. Since the constraint is quadratic in nature, the optimum \mathbf{w} and \mathbf{b} are obtained using an iterative algorithm. See [12] for details.

Note from (2) that all the feedback taps have equal weightage in contributing to the offset at the slicer input. However, in the energy constrained approach, taps with larger magnitudes receive more weightage and, hence, these get suppressed more compared to those with smaller magnitudes. As a result, the taps near the tail tend to get bigger, which is not desirable from EP point of view. To overcome this problem, a more appropriate approach should be to directly control the magnitude of the taps and this leads to a new EP suppression method called “magnitude-constrained design method.” It can be done by constraining the sum of magnitudes of the taps, i.e., $\sum_i |b_i| = \alpha_m$, where α_m is some appropriate positive real number. But $\sum_i |b_i|$ is not differentiable. This difficulty can be easily circumvented in our case as explained below. For channel densities around two to three, all except the first tap in the feedback equalizer (in unconstrained design) are negative, i.e., we know the sign of each b_i *a priori*. Hence, we can write

$$\sum_i |b_i| = b_1 - \sum_{i=2}^{N_b} b_i = \mathbf{u}^T \mathbf{b}$$

where $\mathbf{u} = [1 \ -1 \ -1 \ \dots \ -1]^T$, a vector of N_b elements. Further, by selectively setting some elements of \mathbf{u} to zero, we can select the taps to be included in the constraint. The problem now becomes

$$\min_{\mathbf{w}, \mathbf{b}} P_n(\mathbf{w}, \mathbf{b}) \text{ subject to } \mathbf{u}^T \mathbf{b} = \alpha_m. \quad (4)$$

Using the Lagrange multiplier approach [13], we get the new cost function as

$$J(\mathbf{w}, \mathbf{b}, \lambda) = P_n(\mathbf{w}, \mathbf{b}) + 2\lambda(\mathbf{b}^T \mathbf{u} - \alpha_m)$$

where λ is the Lagrange multiplier. Setting the gradients of $J(\mathbf{w}, \mathbf{b}, \lambda)$ with respect to \mathbf{w} , \mathbf{b} , and λ to zero and solving the system of equations, we get the optimum \mathbf{w} and \mathbf{b} as

$$\begin{aligned} \mathbf{w} &= \mathbf{R}_z^{-1}(\mathbf{R}_{za} \mathbf{b} + \mathbf{r}_{za}) \\ \mathbf{b} &= \mathbf{d} - \lambda \mathbf{C}^{-1} \mathbf{u} \\ \lambda &= \frac{\mathbf{u}^T \mathbf{d} - \alpha_m}{\mathbf{u}^T \mathbf{C}^{-1} \mathbf{u}} \end{aligned} \quad (5)$$

where $\mathbf{C} = \mathbf{R}_a - \mathbf{R}_{za}^T \mathbf{R}_z^{-1} \mathbf{R}_{za}$ and $\mathbf{d} = \mathbf{C}^{-1}(\mathbf{R}_{za}^T \mathbf{R}_z^{-1} \mathbf{r}_{za} - \mathbf{r}_{aa})$.

Fig. 2 compares the equalized channel responses resulting from the constrained and unconstrained design approaches for a Lorentzian channel at user density 2.5 and channel SNR 27 dB using a 20-tap forward equalizer with oversampling factor $L = 2$ and 7-tap feedback equalizer. Fig. 3 compares the corresponding feedback taps. Only the last six feedback taps are included in the constraints. This is because the first tap b_1 is usually quite large and, hence, trying to reduce it significantly would result in large degradation in detection SNR.² On the other hand, one can exploit the fact that b_1 is large to develop techniques for detecting decision errors as we explain in the next section. Further, since the taps at the tail have significant influence on the probability of long bursts, limiting their magnitudes

²Detection SNR is defined as the ratio of the square of the eye level f_0^2 to the sum of variances of channel noise and residual ISI at the slicer input.

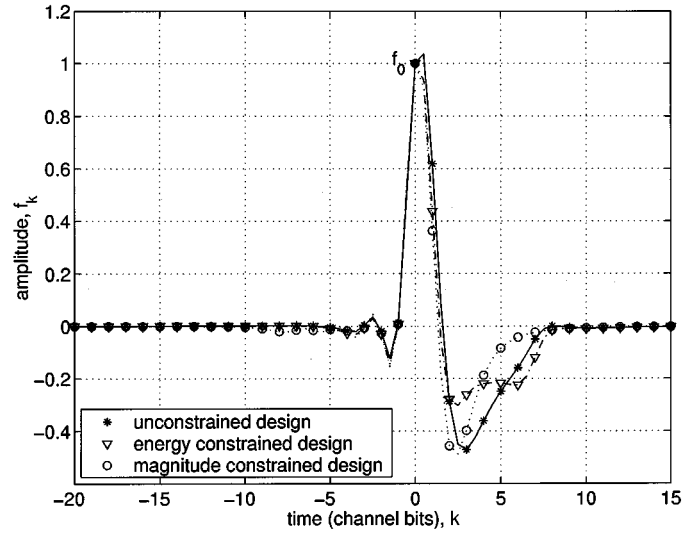


Fig. 2. Equalized channels obtained using constrained and unconstrained design approaches for Lorentzian channel at user density 2.5 (20-tap forward equalizer, 7-tap feedback equalizer, oversampling factor = 2, RLL 16/17 (0,6/6) code, channel SNR = 27 dB, detection SNR = 14.76 dB for constrained design and 15.16 dB for unconstrained design). The constraints are imposed on the last six feedback taps only. The values for energy and sum of magnitudes are $\alpha_e = 0.26$ and $\alpha_m = 1.085$, respectively. Degradation in detection SNR due to constraints is 0.4 dB. Main cursor f_0 is normalized to one in each case.

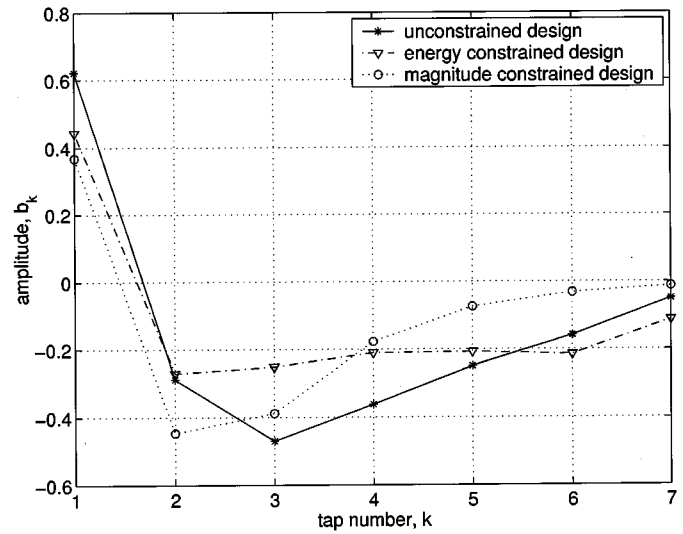


Fig. 3. Feedback tap values resulting from the unconstrained and constrained equalizer design approaches. System parameters are the same as those in Fig. 2. Tap values in each case are normalized by the corresponding main cursor f_0 .

will be more effective in controlling EP. Since the values of α_e and α_m decide the tradeoff between reduction in EP and degradation in detection SNR, we choose these values in such a way that the degradation in detection SNR in the constrained design is 0.4 dB compared to the unconstrained design. This results in $\alpha_e = 0.26$ and $\alpha_m = 1.085$.

Observe from Fig. 3 that, as we expected, the taps in the constrained designs have smaller magnitudes compared to that in the unconstrained design. Further, the values of the taps near the tail are smaller in the case of magnitude constraint compared to energy constraint. This should help in faster decay of error bursts

in the magnitude-constrained case compared to the energy-constrained case. Effectiveness of these constrained approaches in reducing EP is demonstrated in Section V using computer simulations.

III. THRESHOLD TECHNIQUES

As mentioned in Section I, another approach to solving the problem of EP minimization is to detect the presence of decision errors and take measures to prevent/minimize further errors. The threshold techniques developed in this section follow this approach.

Suppose an error event starts at time instant n , i.e., a detection error occurs at instant n and there are no erroneous decisions in the feedback register. The first step (toward EP control) is the detection of the presence of this event, which should be done with minimum delay. We do this by examining the slicer inputs $q(n)$ and $q(n+1)$. There are two reasons for this. First, since the first feedback tap b_1 is always positive and large, it would cause a large offset at the slicer input that can be detected easily. Second, the value of $q(n+1)$ can be well predicted since it is affected by the error at instant n only. On the other hand, the offsets in $q(n+2)$ onwards could be caused by multiple errors, which are much more difficult to deal with.

Since the error event started at instant n , we have $\hat{a}(n-i) = a(n-i)$ for $i = 1, 2, \dots, N_b$ and $\hat{a}(n) = -a(n)$. According to (2), the slicer input at instants n and $n+1$ are

$$q(n) = f_0 a(n) + \eta(n)$$

and

$$q(n+1) = f_0 a(n+1) + \eta(n+1) + 2b_1 a(n) \quad (6)$$

respectively. The error at instant n is solely caused by the channel noise. Hence, most likely, the magnitude of $q(n)$ is quite small. However, the value of $q(n+1)$ would be far from its nominal value f_0 , due to the presence of the $2b_1$ term. Since we did not include b_1 in the constraint during equalizer design, the value of this tap is positive and relatively large. This would provide us a large offset in $q(n+1)$, which makes the detection of error easier. Depending on the relative signs of $a(n)$ and $a(n+1)$, this offset will be different. The two possibilities are considered below.

Case 1— $a(n+1) = a(n)$: In this case

$$q(n) = f_0 a(n) + \eta(n)$$

and

$$q(n+1) = (f_0 + 2b_1)a(n+1) + \eta(n+1). \quad (7)$$

Since $f_0 \approx 1$ and b_1 is relatively large and positive (≈ 0.5), the magnitude of $q(n+1)$ will also be large (> 2) and $\hat{a}(n+1) = a(n+1)$ with probability of one. Since $\hat{a}(n) = -a(n)$, the magnitude of $q(n)$ should be relatively small. Summarizing these, we have the following simple threshold tests for detecting such error events:

$$\left. \begin{array}{l} |q(n)| < \alpha_1 \\ |q(n+1)| > \beta_1 \\ \hat{a}(n) \neq \hat{a}(n+1) \end{array} \right\} \quad (8)$$

where $\alpha_1 = \tilde{\alpha}_1 f_0$ and $\beta_1 = \tilde{\beta}_1 f_0$ with $\tilde{\alpha}_1$ and $\tilde{\beta}_1$ being positive real numbers of the order of 0.5 and 1.5, respectively. The set of threshold tests in (8) are referred to as TT-1 in this paper.

Case 2— $a(n+1) = -a(n)$: In this case

$$q(n) = f_0 a(n) + \eta(n)$$

and

$$q(n+1) = (f_0 - 2b_1)a(n+1) + \eta(n+1). \quad (9)$$

Since $2b_1$ is comparable to f_0 , the magnitude of $q(n+1)$ will be relatively small. Hence, we have the following threshold tests for detecting such error events:

$$\left. \begin{array}{l} |q(n)| < \alpha_2 \\ |q(n+1)| < \beta_2 \end{array} \right\} \quad (10)$$

where $\alpha_2 = \tilde{\alpha}_2 f_0$ and $\beta_2 = \tilde{\beta}_2 f_0$ with $\tilde{\alpha}_2$ and $\tilde{\beta}_2$ being positive real numbers of the order of 0.5. The set of threshold tests in (10) are referred to as TT-2 in this paper.

We may remark here that we do not need the knowledge of $a(n)$ and $a(n+1)$ while using TT-1 or TT-2 for detecting error events. Further, to achieve better detection of error events, TT-1 and TT-2 can be used simultaneously to take care of both the cases. This is because the samples $q(n)$ and $q(n+1)$ will never be able to simultaneously satisfy the threshold tests in TT-1 and TT-2.

Once the presence of an error event has been detected by either of the above tests, the next step is to minimize the possibility of further decision errors. We can do this in two ways. One is to appropriately shift the slicer threshold. If $q(n)$ and $q(n+1)$ pass the threshold tests in TT-1 or TT-2, we assume that a detection error has occurred at time instant n . Then the slicer threshold is shifted from zero to $-\gamma \hat{a}(n)$ at instant $n+1$, where $\gamma = \tilde{\gamma} f_0$ with $0 < \tilde{\gamma} < 1$ since the offset $2b_1 a(n)$ due to the error has the same sign as $a(n)$. On the other hand, since b_i 's are negative for $i = 2, 3, \dots, N_b$, we shift the slicer threshold to $\gamma \hat{a}(n)$ from instants $n+2$ onwards. This special slicer threshold is used until instant $n+N_e$ and it is set back to zero from instant $n+N_e+1$ onwards. The value of N_e is chosen such that the offset $2b_i a(n)$ is not significant for $i > N_e$. Note that a more natural approach would be to use a variable threshold that is proportional to b_i . However, simulations revealed that the BLDs resulting from the use of variable threshold and fixed threshold are quite similar. Hence, we chose the simpler method of fixed threshold. The optimum values of γ and N_e , which result in maximum reduction in EP, can be found through simulations. We denote these parameters by (γ_1, N_{e1}) and (γ_2, N_{e2}) corresponding to TT-1 and TT-2, respectively. Henceforth, this method will be called "threshold-shifting method."

Another way to reduce further errors after detecting an error event is to correct the decision error at instant n , thus leaving the feedback equalizer error free. This is done as follows. If the samples $q(n)$ and $q(n+1)$ satisfy the threshold tests in TT-1 or TT-2, then the decision at instant n is reversed in sign. Using this new decision, say $\hat{a}(n)$, the value of $q(n+1)$ is recalculated and new decision $\hat{a}(n+1)$ for instant $n+1$ is made using this new $q(n+1)$. Thus, the final decision on a bit can only be made after checking the slicer input at the next instant, resulting in a one-bit delay in decisions. This method will be called "error-correction method" in this paper.

IV. THEORETICAL ANALYSIS

The development of the threshold tests in TT-1 and TT-2 are based on the assumption that these tests will be satisfied only in the presence of decision errors. However, large noise fluctuations can also cause these tests to be satisfied even when there are no decision errors. In fact, it may happen that we detect an error event when there is actually none, which we call “false detection,” and we fail to detect an error event when it is present, which we call “detection failure.” Clearly, our method can be considered effective only if the probabilities of false detection and detection failure are sufficiently small. Since these probabilities depend on the values of the threshold parameters α_1 , α_2 , β_1 , and β_2 , these parameters should be chosen to minimize these probabilities. In this section, we derive the equations for computing these probabilities. The purpose of this theoretical analysis is threefold. First, to quantify the effectiveness of TT-1 and TT-2 for a given set of threshold parameters; second, to avoid time consuming simulations for optimizing these parameters; and third, to develop a fast procedure for estimating the overall BLD/BER of a system with error correction.

A. False-Detection Probability

The probability of false detection, denoted as P_f , is the probability of $q(n)$ and $q(n+1)$ passing the threshold tests in (8) or (10) in the absence of decision errors in the feedback register.

First, let us examine TT-1. The false-detection probability for TT-1 is given by

$$P_{f_1} = \Pr[|q(n)| < \alpha_1, |q(n+1)| > \beta_1, \hat{a}(n) \neq \hat{a}(n+1), a(n) = \hat{a}(n), a(n-i) = \hat{a}(n-i) \quad \text{for } i = 1, \dots, N_b]. \quad (11)$$

For the sake of simplicity, we neglect the term $a(n-i) = \hat{a}(n-i)$ for $i = 1, \dots, N_b$ in (11) since the typical BER is of the order of 10^{-6} or less. Thus, we get

$$\begin{aligned} P_{f_1} &= \Pr[|q(n)| < \alpha_1, |q(n+1)| > \beta_1, \hat{a}(n) \neq \hat{a}(n+1), a(n) = \hat{a}(n)] \\ &= 2 \Pr[-+] \cdot \Pr[|q(n)| < \alpha_1, |q(n+1)| > \beta_1, \hat{a}(n) \neq \hat{a}(n+1), a(n) = \hat{a}(n) | -+] \\ &\quad + 2 \Pr[- -] \cdot \Pr[|q(n)| < \alpha_1, |q(n+1)| > \beta_1, \hat{a}(n) \neq \hat{a}(n+1), a(n) = \hat{a}(n) | - -] \end{aligned} \quad (12)$$

where $[-+]$ denotes the event $[a(n) = -1, a(n+1) = +1]$ and $[- -]$ is similarly defined. Now $q(n)$ and $q(n+1)$ can be written as

$$q(n) = f_0 a(n) + f_{-1} a(n+1) + \tilde{\eta}(n)$$

and

$$q(n+1) = f_0 a(n+1) + g_1 a(n) + \tilde{\eta}(n+1) \quad (13)$$

where $\tilde{\eta}(n)$ and $\tilde{\eta}(n+1)$ are such that $\tilde{\eta}(n) + f_{-1} a(n+1) = \eta(n)$, $\tilde{\eta}(n+1) + g_1 a(n) = \eta(n+1)$, and $g_1 = f_1 - b_1$. Since the probabilities in (12) are conditioned upon $a(n)$ and $a(n+1)$, the ISI components $f_{-1} a(n+1)$ and $g_1 a(n)$ are no more random. Further, the conditions $a(n) = \hat{a}(n)$ and $\hat{a}(n) \neq \hat{a}(n+1)$ are equivalent to $q(n) < 0$ and $q(n+1) > 0$, respectively, since

$a(n) = -1$ in (12). Substituting the above and (13) in (12) and also simplifying, we get

$$\begin{aligned} P_{f_1} &= 2 \Pr[-\alpha_1 + f_0 - f_{-1} < \tilde{\eta}(n) < f_0 - f_{-1}, \\ &\quad \tilde{\eta}(n+1) > \beta_1 - f_0 + g_1] \cdot \Pr[-+] \\ &\quad + 2 \Pr[-\alpha_1 + f_0 + f_{-1} < \tilde{\eta}(n) < f_0 + f_{-1}, \\ &\quad \tilde{\eta}(n+1) > \beta_1 + f_0 + g_1] \cdot \Pr[- -]. \end{aligned} \quad (14)$$

Since $\beta_1 + f_0 + g_1$ is large compared to f_0 (see Fig. 2), the second term in (14) is negligibly small compared to the first term. Hence, we get the false-detection probability for TT-1 as

$$P_{f_1} = 2 \Pr[-\alpha_1 + f_0 - f_{-1} < \tilde{\eta}(n) < f_0 - f_{-1}, \tilde{\eta}(n+1) > \beta_1 - f_0 + g_1] \cdot \Pr[-+] \quad (15)$$

For TT-2, the false-detection probability P_{f_2} can be calculated in a similar way. Using the same arguments as that for TT-1, we get

$$\begin{aligned} P_{f_2} &= \Pr[|q(n)| < \alpha_2, |q(n+1)| < \beta_2, a(n) = \hat{a}(n)] \\ &= 2 \Pr[-f_0 - f_{-1} < \tilde{\eta}(n) < \alpha_2 - f_0 - f_{-1}, \\ &\quad -\beta_2 - f_0 - g_1 < \tilde{\eta}(n+1) < \beta_2 - f_0 - g_1] \\ &\quad \cdot \Pr[++] \\ &\quad + 2 \Pr[-f_0 + f_{-1} < \tilde{\eta}(n) < \alpha_2 - f_0 + f_{-1}, \\ &\quad -\beta_2 + f_0 - g_1 < \tilde{\eta}(n+1) < \beta_2 + f_0 - g_1] \\ &\quad \cdot \Pr[+-]. \end{aligned} \quad (16)$$

The expressions in (15) and (16) are evaluated as described below. For the sake of simplicity, we assume the residual ISI to be a Gaussian random variable independent of channel noise. Hence, $\tilde{\eta}(n)$ and $\tilde{\eta}(n+1)$ are jointly Gaussian with variances and covariances given by the sum of the variances and covariances of the channel noise and residual ISI. Since $\tilde{\eta}(n)$ and $\tilde{\eta}(n+1)$ are jointly Gaussian and the pattern probabilities of $a(n)$ and $a(n+1)$ can be estimated by computer simulation, we can easily evaluate the probabilities in (15) and (16).

B. Correct-Detection Probability

The second quantity of interest to us is the probability of detection failure P_{df} or its complement, the probability of correct detection P_c . At time instant n , assume that the feedback register does not contain any erroneous decisions and $a(n)$ is detected wrong. Then, correct-detection probability P_c is the probability that $q(n)$ and $q(n+1)$ pass the threshold tests in this situation. First, let us consider TT-1. In this case, the correct-detection probability is given by

$$P_{c_1} = \Pr[|q(n)| < \alpha_1, |q(n+1)| > \beta_1, \hat{a}(n) \neq \hat{a}(n+1) | a(n) \neq \hat{a}(n), a(n-i) = \hat{a}(n-i) \quad \text{for } i = 1, \dots, N_b].$$

Using similar approximations and manipulations as we did in the case of false-detection-probability computations, we get

$$\begin{aligned} P_{c_1} &= \frac{2}{\Pr[a(n) \neq \hat{a}(n)]} \\ &\quad \times \{ \Pr[|q(n)| < \alpha_1, |q(n+1)| > \beta_1, a(n) \neq \hat{a}(n), \\ &\quad \hat{a}(n) \neq \hat{a}(n+1) | ++] \cdot \Pr[++] \\ &\quad + \Pr[|q(n)| < \alpha_1, |q(n+1)| > \beta_1, a(n) \neq \hat{a}(n), \\ &\quad \hat{a}(n) \neq \hat{a}(n+1) | +-] \cdot \Pr[+-] \}. \end{aligned} \quad (17)$$

Now, $q(n)$ and $q(n+1)$ can be written as

$$q(n) = f_0 a(n) + f_{-1} a(n+1) + \tilde{\eta}(n)$$

and

$$q(n+1) = f_0 a(n+1) + (g_1 + 2b_1) a(n) + \tilde{\eta}(n+1). \quad (18)$$

Further, the conditions $a(n) \neq \hat{a}(n)$ and $\hat{a}(n) \neq \hat{a}(n+1)$ in the numerators of (17) are equivalent to $q(n) < 0$ and $q(n+1) > 0$, respectively, since $a(n) = 1$. Substituting the above and (18) in (17), we get

$$P_{c1} = \frac{2}{\Pr[a(n) \neq \hat{a}(n)]} \times \{ \Pr[-\alpha_1 - f_0 - f_{-1} < \tilde{\eta}(n) < -f_0 - f_{-1}, \tilde{\eta}(n+1) > \beta_1 - f_0 - g_1 - 2b_1] \cdot \Pr[++] + \Pr[-\alpha_1 - f_0 + f_{-1} < \tilde{\eta}(n) < -f_0 + f_{-1}, \tilde{\eta}(n+1) > \beta_1 + f_0 - g_1 - 2b_1] \cdot \Pr[+-] \}. \quad (19)$$

Since the probability of $\tilde{\eta}(n+1) > \beta_1 + f_0 - g_1 - 2b_1$ is very small, the second term in (19) is negligible as compared to the first term. Hence, by dropping this term, we get the correct-detection probability P_{c1} for TT-1 as

$$P_{c1} = 2 \Pr[-\alpha_1 - f_0 - f_{-1} < \tilde{\eta}(n) < -f_0 - f_{-1}, \tilde{\eta}(n+1) > \beta_1 - f_0 - g_1 - 2b_1] \cdot \Pr[+]/\Pr[\eta(n) > f_0]. \quad (20)$$

For TT-2, the correct-detection probability P_{c2} is given by

$$P_{c2} = \frac{\Pr[|q(n)| < \alpha_2, |q(n+1)| < \beta_2 | a(n) \neq \hat{a}(n), a(n-i) = \hat{a}(n-i), i = 1, \dots, N_b]}{2} = \frac{\Pr[a(n) \neq \hat{a}(n)]}{2} \times \{ \Pr[|q(n)| < \alpha_2, |q(n+1)| < \beta_2, a(n) \neq \hat{a}(n)] \cdot \Pr[++] + \Pr[|q(n)| < \alpha_2, |q(n+1)| < \beta_2, a(n) \neq \hat{a}(n)] \cdot \Pr[+-] \}. \quad (21)$$

On carrying out similar manipulations as for TT-1, it turns out that the first term is negligible as compared to the second term. Thus, we get

$$P_{c2} = 2 \Pr[-\alpha_2 - f_0 + f_{-1} < \tilde{\eta}(n) < -f_0 + f_{-1}, -\beta_2 + f_0 - g_1 - 2b_1 < \tilde{\eta}(n+1) < \beta_2 + f_0 - g_1 - 2b_1] \cdot \Pr[+-]/\Pr[\eta(n) > f_0]. \quad (22)$$

The probabilities P_{c1} and P_{c2} can be evaluated using the joint-Gaussian property of $\tilde{\eta}(n)$ and $\tilde{\eta}(n+1)$ and the pattern probabilities of $a(n)$ and $a(n+1)$.

When TT-1 and TT-2 are applied simultaneously, the resulting probabilities of false detection and correct detection are given by the sums of the corresponding individual probabilities for TT-1 and TT-2 since these methods do not occur together.

V. SIMULATION RESULTS

In this section, we present computer simulation results to corroborate the theoretical analysis of Section IV as well as to demonstrate the effectiveness of the approaches proposed in

TABLE I
COMPARISON OF SIMULATION AND THEORETICAL RESULTS FOR FALSE-DETECTION AND CORRECT-DETECTION PROBABILITIES. (THRESHOLD PARAMETERS: $\alpha_1 = 0.15$, $\beta_1 = 1.6$, $\alpha_2 = 0.15$, AND $\beta_2 = 0.4$. CHANNEL SNR = 27 dB)

	False detection probability, P_f		Correct detection probability, P_c	
	TT-1	TT-2	TT-1	TT-2
Simulation	2.9868e-05	6.3215e-05	0.2957	0.3898
Theoretical	3.0007e-05	6.2809e-05	0.3093	0.3883

Sections II and III for reducing EP. The channel and system parameters used in these simulations are as follows. Input data is generated by encoding random binary data using RLL 16/17 (0,6/6) code followed by NRZI modulation. The channel is fractionally spaced ($L = 2$) Lorentzian at user density 2.5. Forward equalizer has 20 taps spaced at T/L and feedback equalizer has seven taps. The equalizer design is done at an SNR of 27 dB.

A. Comparison of Theoretical and Simulation Results

We first present results to corroborate the theoretical analysis. The equalizer design is done without any constraints. The threshold parameters used are $\alpha_1 = 0.15$, $\beta_1 = 1.6$, $\alpha_2 = 0.15$, and $\beta_2 = 0.4$. These parameters were chosen using simulations to achieve good reduction in EP. We used a channel SNR of 22 dB for the simulation. More than 150 million bits were used and about 84 387 error events occurred. Table I shows the values of false-detection probability (P_f) and correct-detection probability (P_c) obtained using simulations and theoretical calculation. Equations (15), (16), (20), and (22) are used for computing the theoretical values. Observe that the theoretical results are very close to the simulation values, in spite of the simplifying approximations used. Thus, for a given set of threshold parameters, the theoretical calculations of P_f and P_c can be used to evaluate the error-event detection performance of TT-1 and TT-2.

Therefore, the theoretical analysis provides us a fast and accurate way to quantify the effectiveness of the threshold tests and to avoid time-consuming simulations for optimizing the threshold parameters. In addition, as we will show later, the values of P_f and P_{df} can be used in conjunction with a fast simulation procedure to obtain the overall BLD and BER of the detector without doing full bit-by-bit simulations. In short, the above theoretical analysis can be used to save a lot of computer time.

B. Constrained Design with Threshold-Shifting Method

Next, we present simulation results to demonstrate the efficacy of the proposed constrained equalizer design approach and threshold-shifting method to reduce EP. The channel SNR was set to 25 dB for the simulation. The values of the parameters α , β , γ , and N_e were chosen by running a few trials. The BLD was estimated using the fast simulation procedure given in [14]. Since the details of this simulation procedure are not available in [14], we have given a brief summary of this algorithm in Appendix I. In the detected bit sequence, an error event is said to begin at instant k_1 and end at instant k_2 if: 1) $\hat{a}(k) \neq a(k)$ for $k = k_1$ and k_2 ; 2) there are no decision errors in N_b bits prior

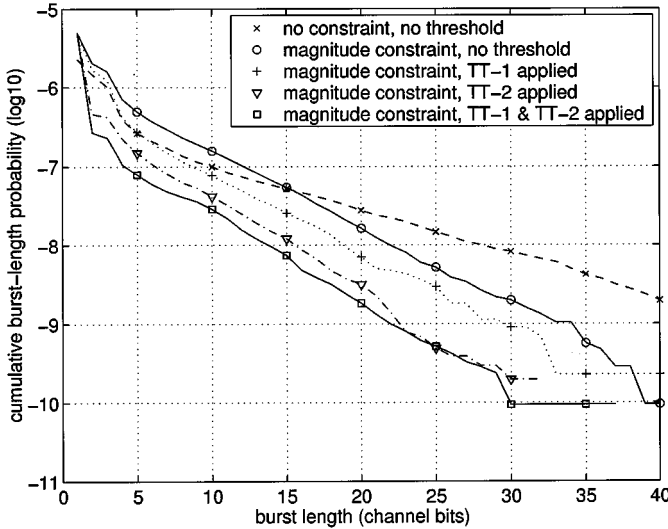


Fig. 4. BLD curves for DFE designed with magnitude constraint and with or without threshold methods at 25-dB channel SNR. System parameters are same as those in Fig. 2. The following threshold parameters are used: $\alpha_1 = 0.15$, $\beta_1 = 1.5$, $\gamma_1 = 0.4$, and $N_{e1} = 4$ for TT-1 and $\alpha_2 = 0.16$, $\beta_2 = 0.42$, $\gamma_2 = 0.4$, and $N_{e2} = 4$ for TT-2. When TT-1 and TT-2 are applied together, the false-detection probability is $P_f = 2.6918e - 06$ and correct-detection probability is $P_c = 0.9281$.

to k_1 and after k_2 ; and 3) there is at least one decision error in any block of N_b bits between k_1 and k_2 .

Fig. 4 shows the BLD curves for magnitude-constrained design with and without the threshold-shifting method. The BLD curves of unconstrained DFE without threshold shifting is also shown for reference. Observe that the constraint helps in almost doubling the slope of the BLD curve compared to the unconstrained design. Further, combining threshold shifting with magnitude constraint results in significant reduction in the probability of error bursts. We may compare these results with Fig. 5, which shows the corresponding curves for energy constrained design. Clearly, the energy constraint also improves the EP performance. However, observe that the magnitude constraint results in a larger decay rate compared to the energy constraint. This, we believe, is the result of having smaller tap values at the tail of the magnitude-constrained feedback equalizer as compared to the energy constrained feedback equalizer (see Fig. 3). Thus, the probability of long error events in the magnitude-constrained case will be smaller than that in the energy constrained case, which is the most desirable feature for an EP reduction scheme.

C. Constrained Design with Error-Correction Method

We see from Fig. 4 that even though the magnitude-constrained design greatly improves the slope of the BLD curve, the loss in detection SNR due to the constraint causes the error event rate to be higher than that of the unconstrained design. However, recall from Section III that the error-correction method can help to reduce the number of error events. Hence, by applying error correction on the magnitude-constrained detector, we can have the good slope produced by the magnitude-constrained design and reduced error event rate due to error correction.

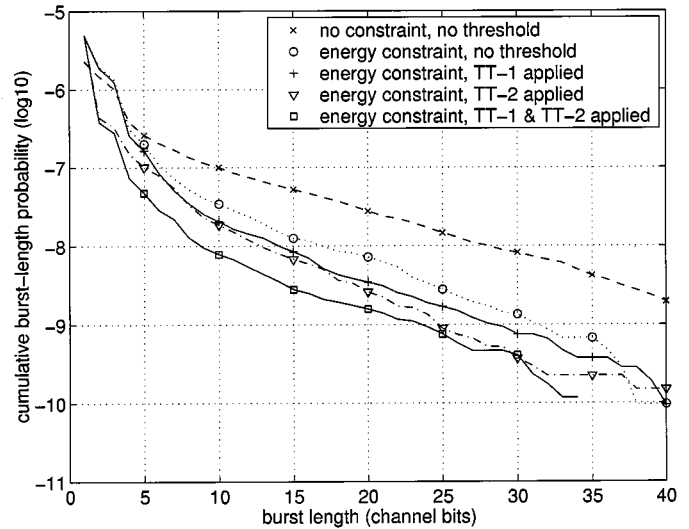


Fig. 5. BLD curves for DFE designed with energy constraint and with or without threshold methods at 25-dB channel SNR. System parameters are same as those in Fig. 2. The following threshold parameters are used: $\alpha_1 = 0.15$, $\beta_1 = 1.6$, $\gamma_1 = 0.5$, and $N_{e1} = 5$ for TT-1 and $\alpha_2 = 0.15$, $\beta_2 = 0.4$, $\gamma_2 = 0.4$, and $N_{e2} = 5$ for TT-2. When TT-1 and TT-2 are applied together, the false-detection probability is $P_f = 1.3005e - 06$ and correct-detection probability is $P_c = 0.9172$.

As before, to save time, we want to use the fast simulation procedure [14] for estimating the BLD curve. However, we need to be cautious while using this method for a system with error correction. We note that the error events generated by the fast method correspond to correct detection and detection failure. No events are generated that correspond to false detection. Nevertheless, this is acceptable in the case of threshold-shifting method since false detection does not necessarily lead to decision errors and because the false-detection probability is sufficiently smaller than error event rate. On the contrary, with error-correction method, false detections surely cause decision errors. Hence, to get reasonably accurate estimate of the overall BLD in this case using the fast procedure, it is necessary to generate events corresponding to not only detection failure but also false detection. Hence, the BLD curves for detection failure and false detection are obtained separately since the injected noise samples have different distributions for these two cases. Note that there is no BLD curve for correct detection here because an error event is always removed should it be correctly detected. The overall BLD curve is given by a weighted sum of these individual BLD curves, the weights being the probabilities of detection failure and false detection. This is another use of the theoretical calculation of P_{df} and P_f . In addition, the BER of the system can also be estimated using the fast algorithm. The average number of errors in an error event can be calculated separately for each case, i.e., detection failure and false detection, by the fast algorithm. The total BER is then calculated by weighing these average numbers of errors by P_{df} and P_f . To verify the above argument, simulations were done for the system with channel SNR equal to 20 dB. Fig. 6 shows the BLD curves of the system with error correction by full simulation and by fast algorithm. As shown, the two curves match each other very well, thus showing that the fast

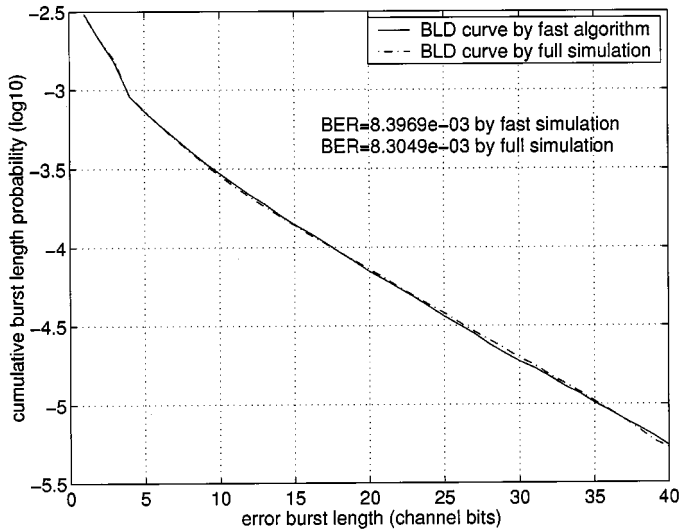


Fig. 6. BLD for DFE detectors with error-correction method obtained using conventional full simulation and the fast algorithm. System parameters are same as those in Fig. 2. Channel SNR used to generate the BLD curves is 20 dB.

algorithm is accurate in estimating the BLD curve for system with error correction. In addition, the BER obtained through full simulation and fast algorithm are very close.

Fig. 7 shows the BLD curve of magnitude-constrained design with error correction. The BLD curves without error correction are also shown for reference. As we noted previously, constrained design results in lower detection SNR, which in turn causes more error events. However, the error-correction method can effectively get rid of many of the error events and, as shown, the resulting error event rate is lower than even that of unconstrained design. Similarly, observe that the BER of constrained design with error correction is lower than that of unconstrained design without error correction. Thus, combining magnitude-constrained design with error-correction method can effectively increase the slope of BLD curve and, at the same time, reduce the BER, both of which are desirable features of a good detection scheme.

Next, we want to compare the performances of threshold-shifting and error-correction methods when applied to magnitude-constrained DFE. The corresponding performances are given by the lower most curves in Figs. 4 and 7. Observe that even though the error event rate in threshold-shifting method is about four times that in error-correction method, it outperforms error-correction method for burst lengths greater than one. This is mainly because of the large drop in the probability from single-bit events to two-bit events. This means that there are a lot of single errors when the threshold-shifting method is used, which is obvious because the EP is effectively stopped by the extra threshold applied. We also see that superiority of threshold-shifting method over error-correction method improves with burst length. Thus, for a given ECC overhead, the threshold-shifting method should be a better choice.

Finally, note that in the constrained equalizer design method, there is a tradeoff between BER and EP, i.e., the gain in EP

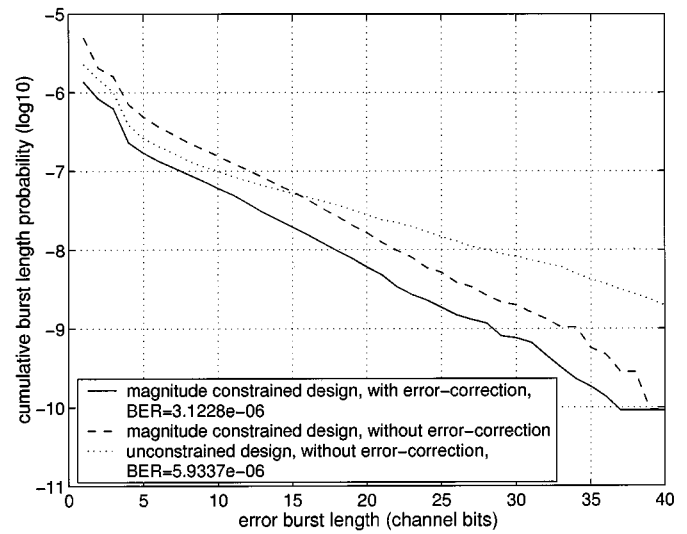


Fig. 7. BLD for magnitude-constrained DFE with or without error correction at 25-dB channel SNR. System parameters are same as those in Fig. 2. The following threshold parameters are used: $\alpha_1 = 0.12$, $\beta_1 = 1.6$, $\alpha_2 = 0.12$, and $\beta_2 = 0.32$. The false-detection probability is $P_f = 4.3048e - 07$ and the probability of detection failure is $P_{df} = 9.2805e - 07$.

suppression comes at the cost of higher BER. On the other hand, the threshold techniques can improve BER and EP simultaneously. In particular, for a given design the threshold-shifting method results in less EP compared to the error-correction method whereas the error-correction method has lower BER. Further, the BER performance of magnitude-constrained system can be improved by supplementing the system with the threshold methods.

Before we conclude this section, we would like to comment on the efficiency of the fast algorithm in reducing the simulation time, which is used for estimating BLD and BER. As an example, at 20-dB SNR the fast approach accumulated about 60 000 error events (20 000 detection failures and 40 000 false detections) in 3.51 h, while the full simulation accumulated about 103 000 events (83 000 detection failures and 20 000 false detections) in 3.73 h. On the other hand, at 25-dB SNR the fast approach performed as at 20 dB while the full simulation could collect only about 900 events in about 167 h. Further, in full simulation, it is much harder to get events corresponding to false detection because of the low false-detection probability. Thus, the saving in computer time provided by the fast approach is very significant and increases exponentially with SNR.

D. Comparison with Existing EP Suppression Methods

To get an idea of how the methods proposed in this paper compare with existing techniques for EP suppression, we did the following. For comparison purpose, we used dual DFE [2], which is proposed for $d = 0$ coded channels, and MDFE [7], [9], [12], which is proposed for $d = 1$ coded channels. Here, “ d ” denotes the minimum run-length constraint. Dual DFE consists of two DFE detectors and is expected to result in less EP compared to single DFE [2]. We did not use any additional techniques to suppress EP in dual DFE. MDFE can be considered as

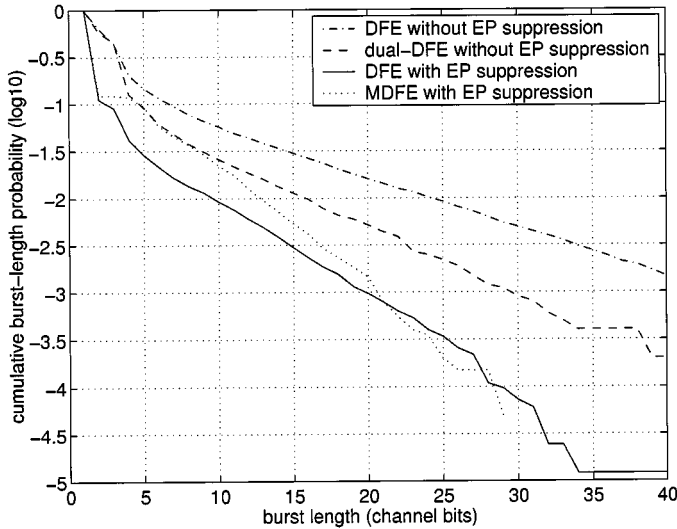


Fig. 8. Normalized BLD curves for DFE, dual DFE, DFE with EP suppression, and MDFE with EP suppression. System parameters in all the detectors are same as those in Fig. 2 except that MDFE uses ten feedback taps. Channel SNR is equal to 22.2 dB for dual DFE, 23.55 dB for DFE, and 24.65 dB for MDFE. In dual DFE, the slicer threshold $\alpha = 0.2$ and the decision delay is $\delta = 10$. The magnitude-constrained design and threshold-shifting method are used in DFE with EP suppression. The energy-constrained design and EP suppression methods proposed in [7] and [9] are used in MDFE. For the method in [9], the number of bits over which the slicer threshold is shifted in the case of a code-constraint violation is three and the new threshold value is 0.8. For the method in [7], the following threshold parameters are used: $\alpha = 0.85$, $\beta = 1.46$, $\gamma = 0.85$, and $N_e = 4$.

DFE optimized for $d = 1$ channels. To suppress EP in MDFE, we use the energy constraint approach proposed in [12] together with the threshold techniques proposed in [7] and [9]. In [9], EP is detected by looking for violation in code constraints. In [7], this is done by looking for samples with large amplitudes at the slicer input. In both these, EP suppression is done by appropriately shifting the slicer threshold. In this study, the system parameters of the different detectors are chosen such that the error event rate without applying any suppression is the same for all the detectors. The value of error event rate is chosen as 5×10^{-5} . The reason for choosing such a high value is to reflect the low SNR situation that will be typical for future high density disk drives. The BLD curves obtained for these detectors are shown in Fig. 8. For comparison purpose, we also give the EP for single DFE without any suppression applied. For the case of DFE with EP suppression, we use the magnitude-constrained design together with the threshold-shifting method. As expected, dual DFE has reduced EP compared to single DFE. However, as can be seen, the DFE with EP suppression proposed in this paper significantly outperforms dual DFE. Further, its performance is also significantly better than that of MDFE for short burst lengths. For large bursts, the trend shows that MDFE will perform the best. The better performance of MDFE for large bursts come from the fact that the technique proposed in [9] is able to detect such bursts by looking for violation in the maximum run length constraint. By supplementing the schemes proposed in this paper with such techniques, we can improve the EP performance of DFE for long bursts.

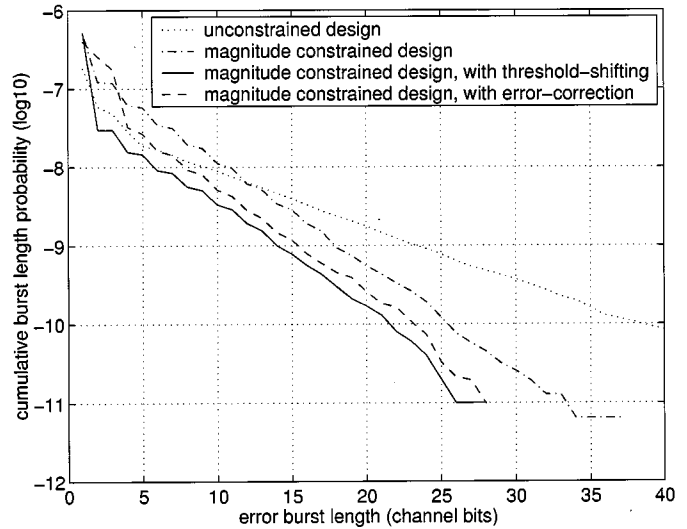


Fig. 9. BLD curves for DFE designed with/without magnitude constraint, with/without threshold shifting, and with/without error correction for Lorentzian channel at user density 2.25 and 25-dB channel SNR [20-tap forward equalizer, 7-tap feedback equalizer, oversampling factor = 2, RLL 16/17 (0,6/6) code, channel SNR = 27 dB for equalizer design]. In the magnitude-constrained design, the sum of magnitudes of the last six taps is $\alpha_m = 0.96$. The detection SNR for the unconstrained and constrained cases are 16.07 dB and 15.67 dB, respectively. Threshold-shifting case: $\alpha_1 = 0.15$, $\beta_1 = 1.3$, $\gamma_1 = 0.5$, $N_{e1} = 5$, $\alpha_2 = 0.13$, $\beta_2 = 0.42$, $\gamma_2 = 0.3$, and $N_{e2} = 5$; false-detection probability $P_f = 2.507e - 07$; and correct-detection probability $P_c = 0.7125$. Error correction case: $\alpha_1 = 0.1$, $\beta_1 = 1.4$, $\alpha_2 = 0.1$, and $\beta_2 = 0.35$; false-detection probability $P_f = 4.8569e - 08$; and correct-detection probability $P_c = 0.5550$.

E. Simulation Results for Other Densities

We may note that all the results presented above are for user density 2.5. In this section, we present some results for different user densities to show that the proposed schemes are effective over the range of typical densities.

Fig. 9 shows the BLD curves for DFE designed with/without magnitude constraint, with/without threshold-shifting, and with/without error correction for Lorentzian channel at user density 2.25. The corresponding set of curves for user density 2.75 are shown in Fig. 10. Note that it may be required to optimize the threshold parameters separately for threshold-shifting and error-correction methods, as shown in Figs. 9 and 10. Also, at high densities (e.g., $D_u = 2.75$), it is required to tighten the constraint to ensure good slope in the BLD curve for applying error correction. This is necessary to ensure reliability with error correction. Hence, we chose to allow a detection SNR loss of 0.7 dB (instead of 0.4 dB) at $D_u = 2.75$ when applying error correction. However, observe that error correction is able to recover this loss in SNR. Thus, we can rely on the error correction method to maintain the error event rate at the level of the original unconstrained level. Finally, as shown in Figs. 9 and 10, the threshold-shifting method is very effective in minimizing EP at the densities considered here.

From Figs. 4, 7, 9, and 10 we may conclude that the proposed magnitude-constrained design and threshold techniques are very effective in minimizing EP for typical user densities of interest. Further, we note that the complexity required to im-

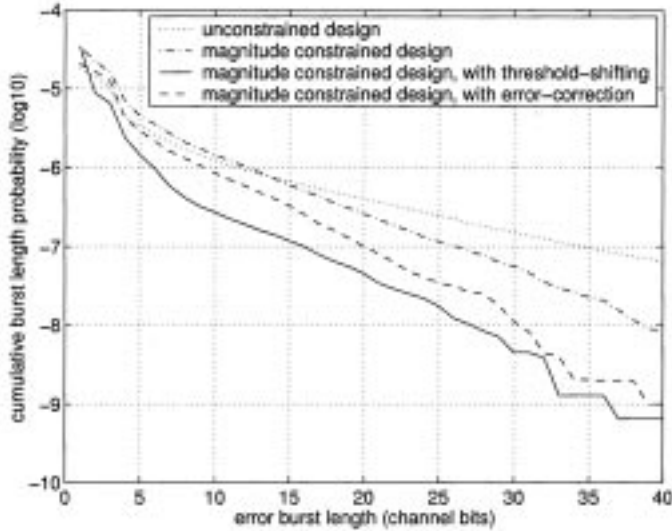


Fig. 10. BLD curves for DFE designed with/without magnitude constraint, with/without threshold shifting, and with/without error correction for Lorentzian channel at user density 2.75 and 25 dB channel SNR [20-tap forward equalizer, 7-tap feedback equalizer, oversampling factor = 2, RLL 16/17 (0,6/6) code, channel SNR = 27 dB for equalizer design]. The detection SNR for unconstrained design is 14.23 dB. Threshold-shifting case: the sum of magnitudes of the last six taps $\alpha_m = 1.2$; detection SNR for constrained design = 13.83 dB; $\alpha_1 = 0.22$, $\beta_1 = 1.66$, $\gamma_1 = 0.4$, $N_{e1} = 5$, $\alpha_2 = 0.16$, $\beta_2 = 0.42$, $\gamma_2 = 0.4$, and $N_{e2} = 3$; false-detection probability $P_f = 1.3271e - 05$; and correct-detection probability $P_c = 0.8257$. Error-correction case: $\alpha_m = 1.05$; detection SNR for constrained design = 13.53 dB; $\alpha_1 = 0.18$, $\beta_1 = 1.5$, $\alpha_2 = 0.12$, and $\beta_2 = 0.3$; false-detection probability $P_f = 6.0033e - 06$; and correct-detection probability $P_c = 0.7530$.

plement the threshold techniques is very minimal since they involve simple threshold tests only. Thus, we may conclude that the combination of constrained-magnitude equalizer design and threshold techniques, which is proposed and studied in this paper, is very much a practically viable scheme and has the potential to significantly reduce the probability of occurrence of long error bursts in DFE detectors.

VI. CONCLUSION

In this paper, two approaches have been proposed for reducing EP in DFE detectors. The first one is a constrained-equalizer design method, which aims to reduce the effect of a detection error on the following bits by constraining the sum of magnitudes of the feedback taps. The second one consists of two novel threshold techniques. These techniques detect the presence of erroneous decisions in the feedback register by examining the slicer input. Upon detection of an error event, either the slicer threshold is appropriately shifted to reduce the possibility of further errors (threshold-shifting method) or the previous error is corrected to make the feedback register error free (error-correction method). Theoretical analysis of the threshold techniques has been carried out to assess the false-detection and correct-detection performances. Simulation results show that combining the constrained equalizer design approach with the threshold techniques results in significant improvement in EP

performance. Further, both these techniques are simple to implement in a practical system.

APPENDIX I

FAST ALGORITHM FOR ERROR PROPAGATION SIMULATION

In this appendix, we give a brief summary of the fast algorithm proposed in [14] for estimating BLD in EP studies of DFE systems. Since the error event rate in magnetic recording channels with reasonable SNRs is of the order of 10^{-6} or less, an accurate estimation of BLD would require very time-consuming simulations. The fast algorithm in [14] circumvents this difficulty by artificially injecting noise samples to generate error events more frequently. The algorithm basically comprises the following two steps.

A. Generation of the First Noise Sample

When the feedback register does not contain any erroneous decisions, the algorithm cuts off the noise from the channel and generates a noise sample to start an error event, i.e., to cause a decision error. Without any loss of generality, we assume $a(n) = -1$. Since the noise samples are of Gaussian distribution, the probability density function of this injected noise sample is given by

$$f_X(x) = \frac{1}{\sqrt{2\pi}\sigma Q(f_0/\sigma)} \exp\left(-\frac{x^2}{2\sigma^2}\right), \quad x \geq f_0 \quad (23)$$

where $Q(y) = 1/\sqrt{2\pi} \int_y^\infty \exp(-x^2/2) dx$ and σ is the variance of the channel noise at slicer input. Whenever a new error event is to be started, the first noise sample is generated according to the above probability density function, which is obviously the tail part of a Gaussian density with the tail beginning at f_0 .

B. Generation of Subsequent Noise Samples

Since the noise samples at the output of the forward equalizer are correlated, we need to inject subsequent noise samples to satisfy this correlation structure. Since the noise samples are jointly Gaussian, the conditional probability density function of the k th injected noise sample is given by

$$f_{X_k|X_1X_2\dots X_{k-1}}(x_k|X_i = x_i, \quad i = 1, 2, \dots, k-1) = \frac{1}{\sqrt{2\pi}\sigma_c} \exp\left(-\frac{(x_k - m_c)^2}{2\sigma_c^2}\right). \quad (24)$$

Here, $m_c = -(\boldsymbol{\eta}^T(k)\mathbf{r}_k/r_{k,0})$ is the conditional mean and $\sigma_c^2 = 1/r_{k,0}$ is the conditional variance, where $\boldsymbol{\eta}(k) = [\eta(n+k-1), \eta(n+k-2), \dots, \eta(n)]^T$ and \mathbf{r}_k and $r_{k,0}$ can be obtained from the following partitioning of the inversion of $(k+1) \times (k+1)$ covariance matrix \mathbf{C}_{k+1} of the equalizer output noise [15]:

$$\mathbf{C}_{k+1}^{-1} = \begin{bmatrix} r_{k,0} & \mathbf{r}_k^T \\ \mathbf{r}_k & \mathbf{R}_k \end{bmatrix}.$$

The noise samples are injected according to the density function (24) until the error event is over. Once the event is over, another event can be started by going back to Step 1.

APPENDIX II
FAST ALGORITHM FOR ERROR PROPAGATION SIMULATION
UNDER FALSE DETECTIONS

The fast algorithm for estimating the BLD that arises from false detections in the threshold techniques proposed in Section III is slightly different from that in Appendix I. In this case, we need to first generate two noise samples so that $q(n)$ and $q(n+1)$ pass the threshold tests and cause a false detection. Below, we explain the procedure developed for doing this.

A. Generation of the First Noise Sample

To produce a false detection, the first and second noise samples must fall into specified ranges. Let these ranges be (l_1, u_1) and (l_2, u_2) for samples 1 and 2, respectively. Since the noise samples are jointly Gaussian, the marginal density of the first noise sample is given by

$$f_{X_1|X_2}(x_1|X_2 \in (l_2, u_2)) = \frac{\int_{l_2}^{u_2} f_{X_1, X_2}(x_1, x_2) dx_2}{\int_{l_1}^{u_1} \int_{l_2}^{u_2} f_{X_1, X_2}(x_1, x_2) dx_2 dx_1}, \quad x_1 \in (l_1, u_1) \quad (25)$$

where

$$f_{X_1, X_2}(x_1, x_2) = \frac{1}{2\pi\sigma^2\sqrt{1-r^2}} \exp\left[-\frac{x_1^2 - 2rx_1x_2 + x_2^2}{2(1-r^2)\sigma^2}\right].$$

σ^2 is the variance of noise samples at the slicer input and r is the normalized covariance of x_1 and x_2 . The first noise sample is generated according to the above conditional density function.

B. Generation of the Second and Subsequent Noise Samples

After the first noise sample is generated, the conditional mean m_c and variance σ_c^2 of the second noise sample can be calculated using the formulas given in Step 2 of Appendix I. The second noise sample is then generated according to the following density function:

$$f_{X_2}(x_2) = \frac{\exp\left(-\frac{(x_2 - m_c)^2}{2\sigma_c^2}\right)}{\int_{l_2}^{u_2} \exp\left(-\frac{(x_2 - m_c)^2}{2\sigma_c^2}\right) dx_2}, \quad x_2 \in (l_2, u_2). \quad (26)$$

The subsequent noise samples are generated in the same way as described in Step 2 of Appendix I.

REFERENCES

- [1] J. J. Moon and L. R. Carley, "Performance comparison of detection methods in magnetic recording," *IEEE Trans. Magn.*, vol. 26, pp. 3155–3172, Nov. 1990.
- [2] J. W. M. Bergmans, J. O. Voorman, and H. W. Wong-Lam, "Dual decision feedback equalizer," *IEEE Trans. Commun.*, vol. 45, pp. 514–518, May 1997.
- [3] K. C. Indukumar, Y. X. Lee, and G. Mathew, "Performance comparison of modified multilevel DFE detectors," *IEEE Trans. Magn.*, vol. 35, pp. 594–604, Jan. 1999.
- [4] M. Russel and J. W. M. Bergmans, "A technique to reduce error propagation in M -ary decision feedback equalization," *IEEE Trans. Commun.*, vol. 43, pp. 2878–2881, Dec. 1995.

- [5] M. Chiani, "Introducing erasures in decision feedback equalization to reduce error propagation," *IEEE Trans. Commun.*, vol. 45, pp. 757–760, July 1997.
- [6] A. Fertner, "Improvement of bit-error-rate in decision feedback equalizer by preventing decision error propagation," *IEEE Trans. Signal Processing*, vol. 46, pp. 1872–1877, July 1998.
- [7] G. Mathew, Y. X. Lee, and V. Y. Krachkovsky, "A novel threshold technique for minimizing error propagation in MDFE read channel," in *Proc. IEEE GLOBECOM Conf.*, Sydney, Australia, Nov. 1998, pp. 2898–2903.
- [8] H. Ueno, "Suppression method for error propagation on MDFE," presented at the 2nd MDFE Consortium Meet., Akita, Japan, Oct. 1997.
- [9] H. Ueno, T. Suguwara, K. Shimoda, and H. Mutoh, "A method for suppressing error propagation in (1,7) MDFE detectors," *IEEE Trans. Magn.*, vol. 35, pp. 2289–2291, Sept. 1999.
- [10] N. Likhonov, Y. X. Lee, and G. Mathew, "Error propagation suppression in MDFE and M2DFE detectors," presented at the 4th MDFE Consortium Meeting, Singapore, Apr. 1998.
- [11] M. Y. Lin, V. Y. Krachkovsky, and G. Mathew, "Conditional ML and MAP techniques for error propagation suppression in multipath DFE detectors," presented at the Dig. INTERMAG 2000 Conf., Toronto, Canada, Apr. 2000.
- [12] G. Mathew, B. Farhang-Boroujeny, R. W. Wood, and B. Liu, "Constrained equalizer design for MDFE detection on the magnetic recording channel," in *Proc. IEEE GLOBECOM Conf.*, Phoenix, AZ, Nov. 1997, pp. 1258–1262.
- [13] A. Jeffrey, *Mathematics for Engineers and Scientists*, 4th ed, New York: Van Nostrand, 1989, pp. 572–578.
- [14] V. Y. Krachkovsky, Y. X. Lee, G. Mathew, and M. Y. Lin, "Fast prediction of error propagation in DFE detectors," in *Dig. 7th Joint MMM-Intermag. Conf.*, San Francisco, CA, Jan. 1998, p. 210.
- [15] M. S. Srivastava and E. M. Carter, *An Introduction to Applied Multivariate Statistics*. New York: North-Holland, 1983, pp. 25–35.

Fang Zhao received the B.E. degree in electrical engineering from the National University of Singapore, Singapore, in 2000. She is currently working toward the Master's degree in electrical engineering at the same university.

Her research interests include turbo codes and signal processing in magnetic recording.

George Mathew received the B.E. degree in electronics and communication engineering from the Karnataka Regional Engineering College, Surathkal, India, in 1987, and the M.Sc.(Eng.) and Ph.D. degrees in electrical communication engineering from the Indian Institute of Science, Bangalore, India, in 1989 and 1994, respectively.

He was a Research Associate at the Indian Institute of Science from 1994 to 1995 and a Postdoctoral Fellow at the National University of Singapore, Singapore, from 1995 to 1996. Since 1996, he has been with the Data Storage Institute, Singapore, where he is currently Assistant Manager of the Coding and Signal Processing Department. His research interests include signal processing and magnetic recording.

B. Farhang-Boroujeny received the B.Sc. degree in electrical engineering from Teheran University, Iran, in 1976, the M.Eng. degree in system test technology from University of Wales Institute of Science and Technology, U.K., in 1977, and the Ph.D. degree from Imperial College, University of London, U.K., in 1981.

From 1981 to 1989, he was with the Isfahan University of Technology, Isfahan, Iran. Since 1989, he has been with the National University of Singapore, Singapore. He has authored or coauthored more than 70 scientific papers in international journals and conferences and is the author of the book *Adaptive Filters: Theory and Applications* (New York: Wiley, 1998). His current scientific interests are adaptive signal processing, data transmission, and magnetic recording.

Dr. Farhang-Boroujeny received the 1987 UNESCO Regional Office of Science and Technology for South and Central Asia young scientists award in recognition of his outstanding contribution in the field of computer applications and informatics.